

Probing small- x helicity and OAM distributions in particle production at RHIC and EIC

YURI KOVCHEGOV
THE OHIO STATE UNIVERSITY



Credits

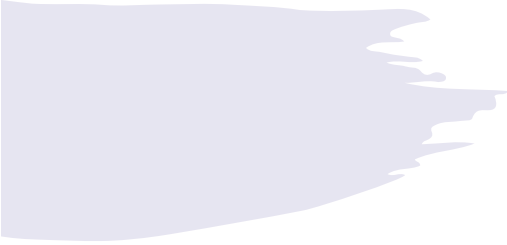
- Based on work done with Dan Pitonyak and Matt Sievert (2015-2018, 2021-present), Florian Cougoulic (2019-present), Gabe Santiago (2020-present), Josh Tawabutr (2020-present), Andrey Tarasov (2021-present), Daniel Adamiak, Wally Melnitchouk, Nobuo Sato (2021-present), Jeremy Borden (2023-present), Ming Li (2023-present), Brandon Manley (2023-present), Nick Baldonado (2022-present), Zardo Becker (2024-present).

Happy 60th
Birthday,
Edmond!



Outline: helicity-dependent observables at RHIC and EIC at small x

- DIS: g_1 structure function at small x + sub-eikonal operators.
- Helicity evolution at small x.
- Polarized DIS and SIDIS data analysis.
- Polarized p+p collisions: gluon production at mid-rapidity.
- Inclusive dijet production in polarized e+p collisions.
- Elastic dijet production in polarized e+p collisions.



g_1 Structure Function

Dipole picture of DIS

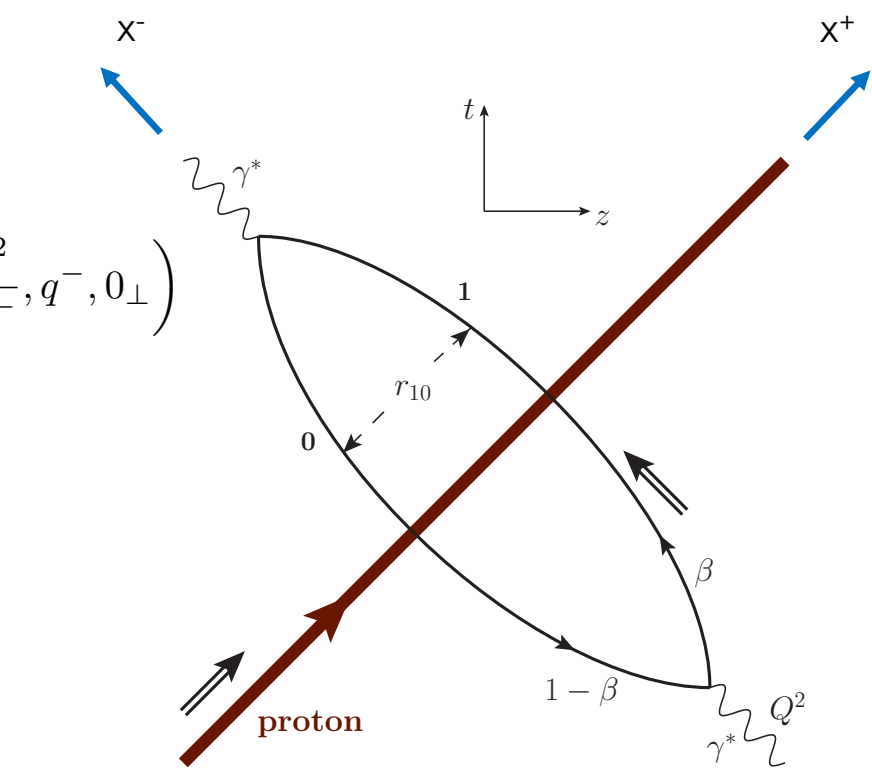
$$W^{\mu\nu} = \frac{1}{4\pi M_p} \int d^4x e^{iq \cdot x} \langle P | j^\mu(x) j^\nu(0) | P \rangle$$

Large $q^- \rightarrow$ large x^- separation

$$q^\mu = \left(\frac{Q^2}{2q^-}, q^-, 0_\perp \right)$$

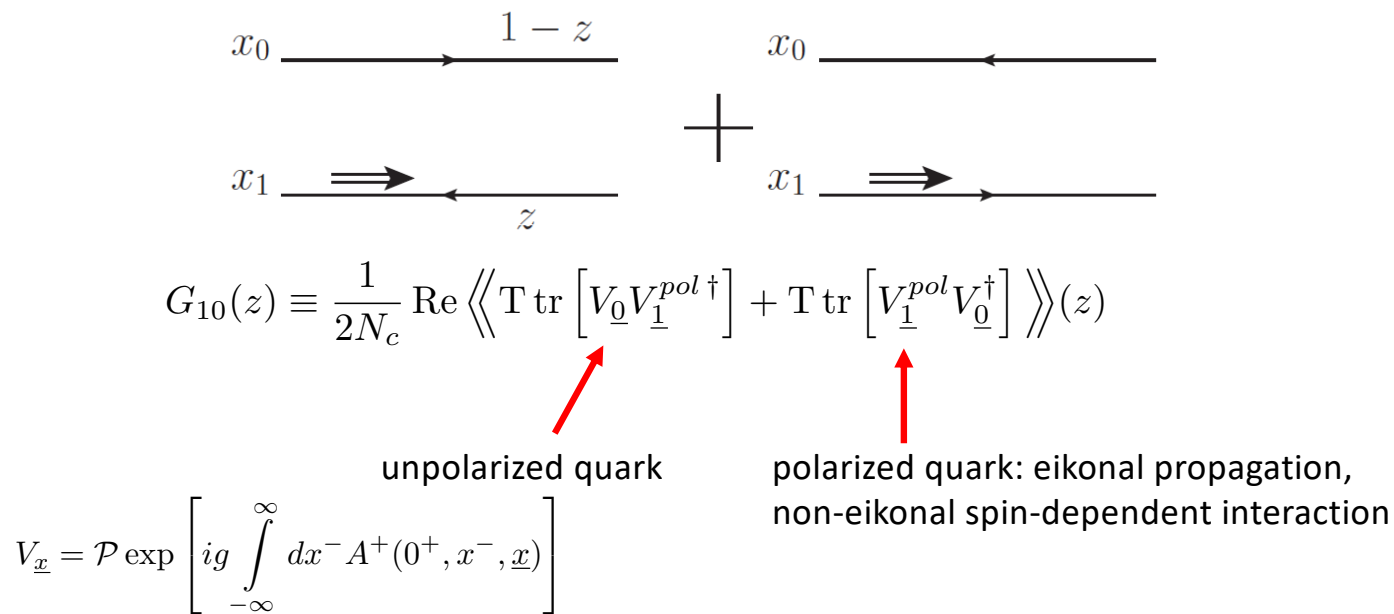
$$e^{iq \cdot x} = e^{i \frac{Q^2}{2q^-} x^- + iq^- x^+}$$

$$x^\pm = \frac{t \pm z}{\sqrt{2}}$$



Polarized Dipole: non-eikonal small-x physics

- All flavor-singlet small- x helicity observables depend on “polarized dipole amplitudes”:

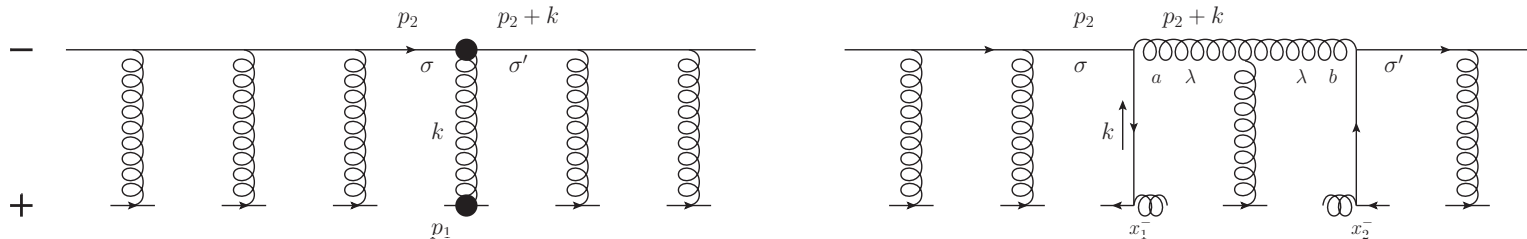


- Double brackets denote an object with energy suppression scaled out:

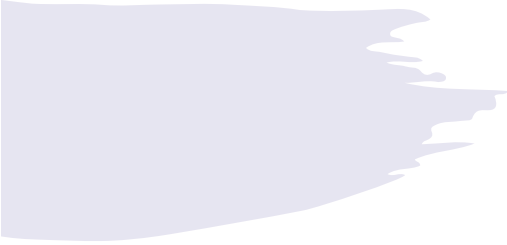
$$\langle\!\langle \mathcal{O} \rangle\!\rangle(z) \equiv z s \langle \mathcal{O} \rangle(z)$$

Polarized fundamental “Wilson line”

- To complete the definition of the polarized dipole amplitude, we need to construct the definition of the polarized “Wilson line” V^{pol} , which is the leading helicity-dependent contribution for the quark scattering amplitude on a longitudinally-polarized target proton.



- At the leading order we can either exchange one non-eikonal t -channel gluon (with quark-gluon vertices denoted by blobs above) to transfer polarization between the projectile and the target, or two t -channel quarks, as shown above.
- We employ a blend of Brodsky & Lepage's LCPT and background field method-inspired operator treatment. We refer to the latter as the **light-cone operator treatment (LCOT)**.



Notation

- Fundamental light-cone Wilson line:

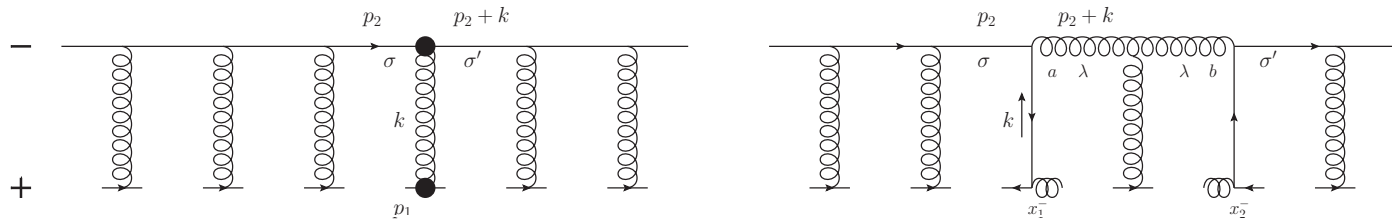
$$V_{\underline{x}}[b^-, a^-] = \text{P exp} \left\{ ig \int_{a^-}^{b^-} dx^- A^+(x^-, \underline{x}) \right\}$$

- Adjoint light-cone Wilson line:

$$U_{\underline{x}}[b^-, a^-] = \mathcal{P} \exp \left[ig \int_{a^-}^{b^-} dx^- \mathcal{A}^+(x^+ = 0, x^-, \underline{x}) \right]$$

- They sum multiple eikonal re-scatterings to all orders.

Sub-eikonal quark S-matrix in background gluon and quark fields



- The full sub-eikonal S-matrix for massless quarks is (Balitsky&Tarasov '15; KPS '17; YK, Sievert, '18; Chirilli '18; Altinoluk et al, '20; YK, Santiago '21)

$$\begin{aligned}
& V_{\underline{x}, \underline{y}; \sigma', \sigma} = V_{\underline{x}} \delta^2(\underline{x} - \underline{y}) \delta_{\sigma, \sigma'} \\
& + \frac{i P^+}{s} \int_{-\infty}^{\infty} dz^- d^2 z V_{\underline{x}}[\infty, z^-] \delta^2(\underline{x} - \underline{z}) \left[-\delta_{\sigma, \sigma'} \overset{\leftarrow}{D}^i D^i + g \sigma \delta_{\sigma, \sigma'} F^{12} \right](z^-, \underline{z}) V_{\underline{y}}[z^-, -\infty] \delta^2(\underline{y} - \underline{z}) \\
& - \frac{g^2 P^+}{2s} \delta^2(\underline{x} - \underline{y}) \int_{-\infty}^{\infty} dz_1^- \int_{z_1^-}^{\infty} dz_2^- V_{\underline{x}}[\infty, z_2^-] t^b \psi_\beta(z_2^-, \underline{x}) U_{\underline{x}}^{ba}[z_2^-, z_1^-] [\delta_{\sigma, \sigma'} \gamma^+ - \sigma \delta_{\sigma, \sigma'} \gamma^+ \gamma^5]_{\alpha\beta} \bar{\psi}_\alpha(z_1^-, \underline{x}) t^a V_{\underline{x}}[z_1^-, -\infty]
\end{aligned}$$

“helicity independent” “helicity dependent” $-\vec{\mu} \cdot \vec{B} = -\mu_z B_z = \mu_z F^{12}$
 “helicity independent” “helicity dependent”

Gluon Helicity

- A calculation gives

$$\Delta G(x, Q^2) = \frac{2N_c}{\alpha_s \pi^2} \left[\left(1 + x_{10}^2 \frac{\partial}{\partial x_{10}^2} \right) G_2 \left(x_{10}^2, zs = \frac{Q^2}{x} \right) \right]_{x_{10}^2 = \frac{1}{Q^2}}$$

$$g_{1L}^{G\,dip}(x, k_T^2) = \frac{N_c}{\alpha_s 2\pi^4} \int d^2 x_{10} e^{-i\underline{k} \cdot \underline{x}_{10}} \left[1 + x_{10}^2 \frac{\partial}{\partial x_{10}^2} \right] G_2 \left(x_{10}^2, zs = \frac{Q^2}{x} \right)$$

- Here we defined a new dipole amplitude G_2 (cf. Hatta et al, 2016; KPS 2017)

$$\int d^2 \left(\frac{x_1 + x_0}{2} \right) G_{10}^i(zs) = (x_{10})_\perp^i G_1(x_{10}^2, zs) + \epsilon^{ij} (x_{10})_\perp^j G_2(x_{10}^2, zs)$$

$$G_{10}^j(zs) \equiv \frac{1}{2N_c} \langle\langle \text{tr} \left[V_0^\dagger V_1^{j\,G[2]} + \left(V_1^{j\,G[2]} \right)^\dagger V_0 \right] \rangle\rangle$$

What is this D-D operator? Turns out it is related to the DD operator from before.

$$V_{\underline{z}}^{i\,G[2]} \equiv \frac{P^+}{2s} \int_{-\infty}^{\infty} dz^- V_{\underline{z}}[\infty, z^-] \left[D^i(z^-, \underline{z}) - \overleftarrow{D}^i(z^-, \underline{z}) \right] V_{\underline{z}}[z^-, -\infty]$$

Quark Helicity PDF and TMD

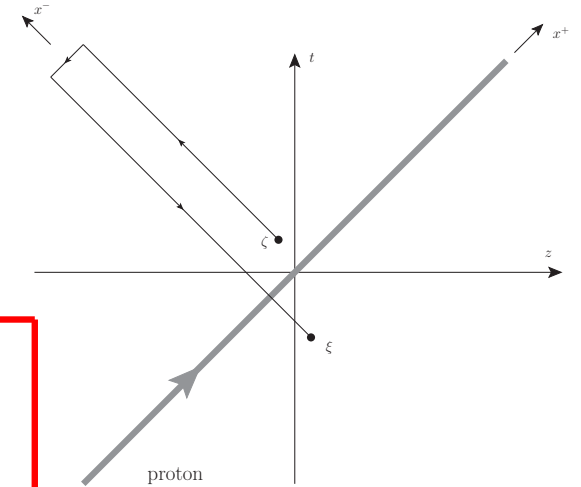
- The flavor-singlet quark helicity PDF and TMD are

$$\Delta\Sigma(x, Q^2) = \frac{N_f}{\alpha_s \pi^2} \tilde{Q} \left(x_{10}^2 = \frac{1}{Q^2}, s = \frac{Q^2}{x} \right)$$

$$g_{1L}^S(x, k_T^2) = \frac{1}{4\pi^4 \alpha_s} \int d^2 x_{10} e^{-i\vec{k} \cdot \vec{x}_{10}} \tilde{Q}(x_{10}^2, Q^2/x)$$

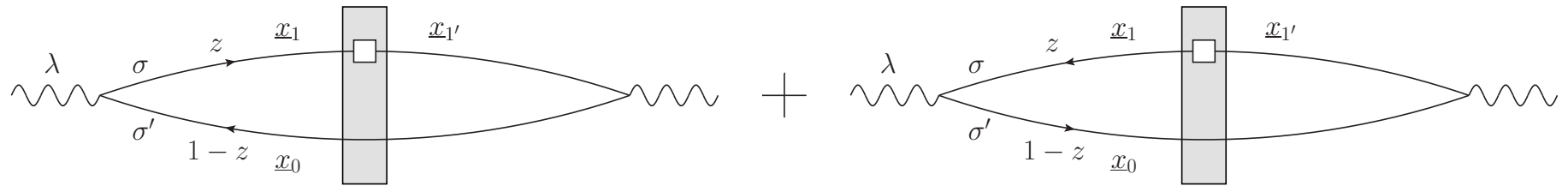
- We have defined another operator:

$$\begin{aligned} \tilde{Q}_{12}(s) \equiv & \left\langle \left\langle \frac{g^2}{16\sqrt{k^- p_2^-}} \int_{-\infty}^{\infty} dy^- \int_{-\infty}^{\infty} dz^- \left[\bar{\psi}(y^-, \underline{x}_2) \left(\frac{1}{2} \gamma^+ \gamma^5 \right) V_2[y^-, \infty] V_1[\infty, z^-] \psi(z^-, \underline{x}_1) \right. \right. \right. \\ & \left. \left. \left. + \bar{\psi}(y^-, \underline{x}_2) \left(\frac{1}{2} \gamma^+ \gamma^5 \right) V_2[y^-, -\infty] V_1[-\infty, z^-] \psi(z^-, \underline{x}_1) + \text{c.c.} \right] \right\rangle \right\rangle (s). \end{aligned}$$



g_1 structure function

- g_1 structure function is obtained similarly, using DIS in the dipole picture:



- One gets

$$g_1(x, Q^2) = - \sum_f \frac{N_c Z_f^2}{4\pi^3} \int_{\Lambda^2/s}^1 \frac{dz}{z} \int_{\frac{1}{zs}}^{\min\left\{\frac{1}{zQ^2}, \frac{1}{\Lambda^2}\right\}} \frac{dx_{10}^2}{x_{10}^2} [Q(x_{10}^2, zs) + 2G_2(x_{10}^2, zs)]$$

- G_2 was defined before. This is the gluon PDF contribution to g_1 .
- The dipole amplitude Q is due to F^{12} & axial current.
- The contribution of G_2 comes from the DD operator in the quark S-matrix.

Amplitude Q

$$Q(x_{10}^2, zs) \equiv \int d^2 \left(\frac{x_0 + x_1}{2} \right) Q_{10}(zs)$$

- The amplitude Q is defined by

$$Q_{10}(zs) \equiv \frac{1}{2N_c} \text{Re} \left\langle \left\langle T \text{tr} \left[V_{\underline{0}} V_{\underline{1}}^{\text{pol}[1]\dagger} \right] + T \text{tr} \left[V_{\underline{1}}^{\text{pol}[1]} V_{\underline{0}}^\dagger \right] \right\rangle \right\rangle$$

with $V_{\underline{x}}^{\text{pol}[1]} = V_{\underline{x}}^{\text{G}[1]} + V_{\underline{x}}^{\text{q}[1]}$, where

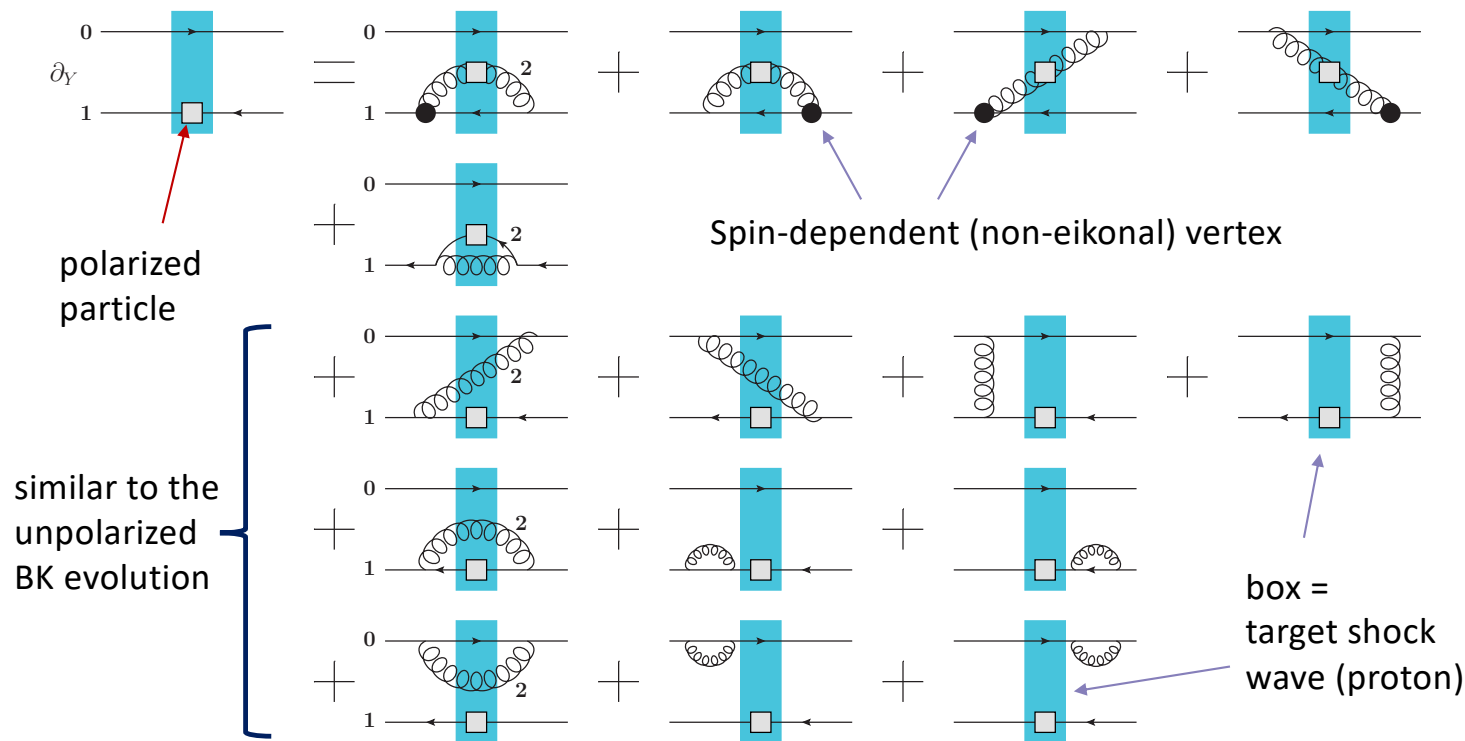
$$V_{\underline{x}}^{\text{G}[1]} = \frac{i g P^+}{s} \int_{-\infty}^{\infty} dx^- V_{\underline{x}}[\infty, x^-] F^{12}(x^-, \underline{x}) V_{\underline{x}}[x^-, -\infty]$$

$$V_{\underline{x}}^{\text{q}[1]} = \frac{g^2 P^+}{2s} \int_{-\infty}^{\infty} dx_1^- \int_{x_1^-}^{\infty} dx_2^- V_{\underline{x}}[\infty, x_2^-] t^b \psi_\beta(x_2^-, \underline{x}) U_{\underline{x}}^{ba}[x_2^-, x_1^-] [\gamma^+ \gamma^5]_{\alpha\beta} \bar{\psi}_\alpha(x_1^-, \underline{x}) t^a V_{\underline{x}}[x_1^-, -\infty]$$

- U = adjoint light-cone Wilson line.
- Summary: we have dipole amplitudes Q and G_2 . We also have \tilde{Q} , but it can be expressed in terms of Q and G_2 after one step of evolution.

Evolution for Polarized Quark Dipole

One can construct an evolution equation for the polarized dipole:



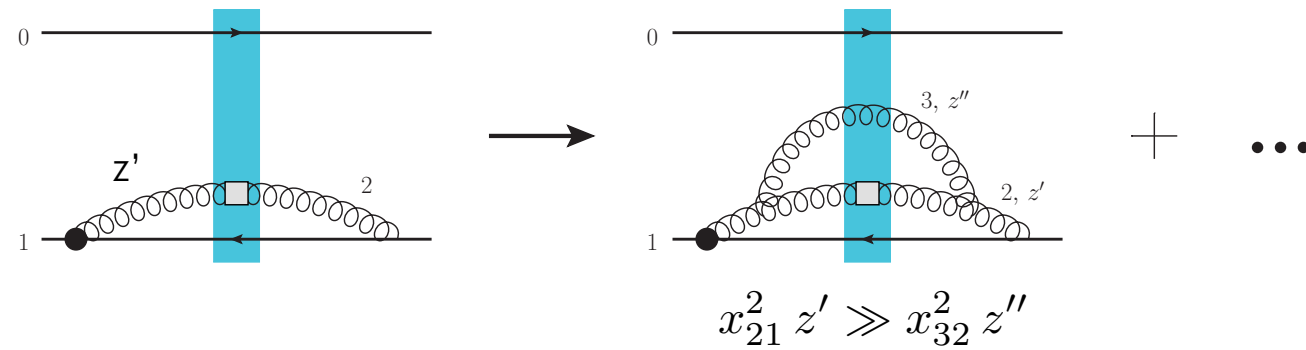
Large N_c Evolution:

- At large-N_c the equations close (Q → G).
- Initial version by YK, D. Pitonyak, M. Sievert '15-'18 (KPS), terms with subscript 2 due to YK, F. Cougoulic, A. Tarasov, Y. Tawabutr '22

$$\begin{aligned}
G(x_{10}^2, zs) &= G^{(0)}(x_{10}^2, zs) + \frac{\alpha_s N_c}{2\pi} \int_{\frac{1}{sx_{10}^2}}^z \frac{dz'}{z'} \int_{\frac{1}{z's}}^{\frac{x_{10}^2}{x_{21}^2}} \frac{dx_{21}^2}{x_{21}^2} \left[\Gamma(x_{10}^2, x_{21}^2, z's) + 3G(x_{21}^2, z's) \right. \\
&\quad \left. + 2G_2(x_{21}^2, z's) + 2\Gamma_2(x_{10}^2, x_{21}^2, z's) \right], \\
\Gamma(x_{10}^2, x_{21}^2, z's) &= G^{(0)}(x_{10}^2, z's) + \frac{\alpha_s N_c}{2\pi} \int_{\frac{1}{sx_{10}^2}}^{z'} \frac{dz''}{z''} \int_{\frac{1}{z''s}}^{\min[x_{10}^2, x_{21}^2, \frac{z'}{z''}]} \frac{dx_{32}^2}{x_{32}^2} \left[\Gamma(x_{10}^2, x_{32}^2, z''s) + 3G(x_{32}^2, z''s) \right. \\
&\quad \left. + 2G_2(x_{32}^2, z''s) + 2\Gamma_2(x_{10}^2, x_{32}^2, z''s) \right], \\
G_2(x_{10}^2, zs) &= G_2^{(0)}(x_{10}^2, zs) + \frac{\alpha_s N_c}{\pi} \int_{\frac{\Lambda^2}{s}}^z \frac{dz'}{z'} \int_{\max[x_{10}^2, \frac{1}{z's}]}^{\min[\frac{z}{z'}x_{10}^2, \frac{1}{\Lambda^2}]} \frac{dx_{21}^2}{x_{21}^2} [G(x_{21}^2, z's) + 2G_2(x_{21}^2, z's)], \\
\Gamma_2(x_{10}^2, x_{21}^2, z's) &= G_2^{(0)}(x_{10}^2, z's) + \frac{\alpha_s N_c}{\pi} \int_{\frac{\Lambda^2}{s}}^{z' \frac{x_{21}^2}{x_{10}^2}} \frac{dz''}{z''} \int_{\max[x_{10}^2, \frac{1}{z''s}]}^{\min[\frac{z'}{z''}x_{21}^2, \frac{1}{\Lambda^2}]} \frac{dx_{32}^2}{x_{32}^2} [G(x_{32}^2, z''s) + 2G_2(x_{32}^2, z''s)]
\end{aligned}$$

“Neighbor” dipole

- There is a new object in the evolution equation – **the neighbor dipole amplitude**.
- This is specific for the DLA evolution. Gluon emission may happen in one dipole, but, due to lifetime ordering, may ‘know’ about another dipole:



- We denote the evolution in the neighbor dipole 02 by $\Gamma_{02, 21}(z')$

A Tale of Two Intercepts

$$\Delta\Sigma(x, Q^2) \Big|_{x \ll 1} \sim \Delta G(x, Q^2) \Big|_{x \ll 1} \sim \left(\frac{1}{x}\right)^{\alpha_h}$$

- Analytic solution of the large- N_c evolution was found in J. Borden, YK, 2304.06161 [hep-ph].
- J. Bartels, B. Ermolaev, and M. Ryskin (BER, 1996) used IR evolution equations to get:

$$\alpha_h = \sqrt{\frac{17 + \sqrt{97}}{2}} \sqrt{\frac{\alpha_s N_c}{2\pi}} \approx 3.664 \sqrt{\frac{\alpha_s N_c}{2\pi}}$$

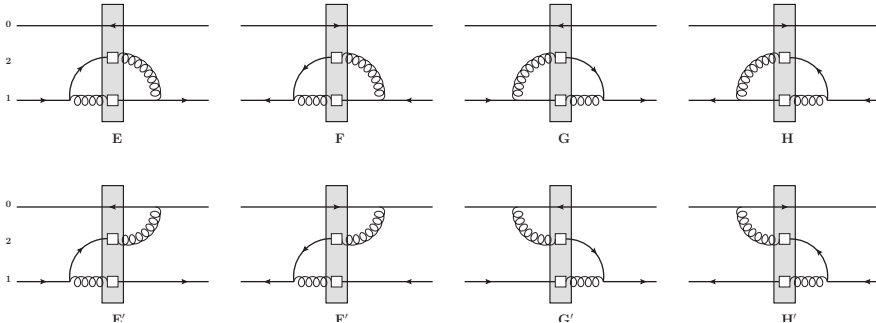
- Us:
$$\alpha_h = \frac{4}{3^{1/3}} \sqrt{\text{Re} \left[(-9 + i\sqrt{111})^{1/3} \right]} \sqrt{\frac{\alpha_s N_c}{2\pi}} \approx 3.661 \sqrt{\frac{\alpha_s N_c}{2\pi}}$$

- Our numerical solution from 2022 also gave the intercept of 3.660 or 3.661, but we believed we had larger error bars.
- We (still) disagree with BER. Albeit in the 3rd decimal point...

Large N_c & N_f Evolution Equations

Initial version by YK, D. Pitonyak, M. Sievert
 '15-'18 (KPS), modifications with subscript 2 due
 to YK, F. Cougoulic, A. Tarasov, Y. Tawabutr '22.

Beyond large- N_c , one needs to add the quark-to-gluon and gluon-to-quark transitions (G. Chirilli, 2101.12744 [hep-ph]; J. Borden, YK, M. Li, 2406.11647 [hep-ph]):



This results in the large- N_c & N_f evolution equations given here (transition terms are in blue). Agrees with DGLAP anomalous dimensions to 3 known loops.

$$Q(x_{10}^2, zs) = Q^{(0)}(x_{10}^2, zs) + \frac{\alpha_s N_c}{2\pi} \int_{1/sx_{10}^2}^z \frac{dz'}{z'} \int_{1/z's}^{x_{10}^2} \frac{dx_{21}^2}{x_{21}^2} \left[2\tilde{G}(x_{21}^2, z's) + 2\tilde{\Gamma}(x_{10}^2, x_{21}^2, z's) \right] \quad (76a)$$

$$+ Q(x_{21}^2, z's) - \bar{\Gamma}(x_{10}^2, x_{21}^2, z's) + 2\Gamma_2(x_{10}^2, x_{21}^2, z's) + 2G_2(x_{21}^2, z's)]$$

$$+ \frac{\alpha_s N_c}{4\pi} \int_{\Lambda^2/s}^z \frac{dz'}{z'} \int_{1/z's}^{\min\{x_{10}^2 z'/z', 1/\Lambda^2\}} \frac{dx_{21}^2}{x_{21}^2} [Q(x_{21}^2, z's) + 2G_2(x_{21}^2, z's)],$$

$$\bar{\Gamma}(x_{10}^2, x_{21}^2, z's) = Q^{(0)}(x_{10}^2, z's) + \frac{\alpha_s N_c}{2\pi} \int_{1/sx_{10}^2}^{z'} \frac{dz''}{z''} \int_{1/z''s}^{\min\{x_{10}^2 z'/z'', 1/\Lambda^2\}} \frac{dx_{32}^2}{x_{32}^2} \left[2\tilde{G}(x_{32}^2, z''s) \right] \quad (76b)$$

$$+ 2\tilde{\Gamma}(x_{10}^2, x_{32}^2, z''s) + Q(x_{32}^2, z''s) - \bar{\Gamma}(x_{10}^2, x_{32}^2, z''s) + 2\Gamma_2(x_{10}^2, x_{32}^2, z''s) + 2G_2(x_{32}^2, z''s)]$$

$$+ \frac{\alpha_s N_c}{4\pi} \int_{\Lambda^2/s}^{z'} \frac{dz''}{z''} \int_{1/z''s}^{\min\{x_{21}^2 z'/z'', 1/\Lambda^2\}} \frac{dx_{32}^2}{x_{32}^2} [Q(x_{32}^2, z''s) + 2G_2(x_{32}^2, z''s)],$$

$$\tilde{G}(x_{10}^2, zs) = \tilde{G}^{(0)}(x_{10}^2, zs) + \frac{\alpha_s N_c}{2\pi} \int_{1/sx_{10}^2}^z \frac{dz'}{z'} \int_{1/z's}^{x_{10}^2} \frac{dx_{21}^2}{x_{21}^2} \left[3\tilde{G}(x_{21}^2, z's) + \tilde{\Gamma}(x_{10}^2, x_{21}^2, z's) \right] \quad (76c)$$

$$+ 2G_2(x_{21}^2, z's) + \left(2 - \frac{N_f}{2N_c} \right) \Gamma_2(x_{10}^2, x_{21}^2, z's) - \frac{N_f}{4N_c} \bar{\Gamma}(x_{10}^2, x_{21}^2, z's) - \frac{N_f}{2N_c} \tilde{Q}(x_{21}^2, z's)]$$

$$- \frac{\alpha_s N_f}{8\pi} \int_{\Lambda^2/s}^z \frac{dz'}{z'} \int_{\max\{x_{10}^2, 1/z's\}}^{\min\{x_{10}^2 z'/z', 1/\Lambda^2\}} \frac{dx_{21}^2}{x_{21}^2} [Q(x_{21}^2, z's) + 2G_2(x_{21}^2, z's)],$$

$$\tilde{\Gamma}(x_{10}^2, x_{21}^2, z's) = \tilde{G}^{(0)}(x_{10}^2, z's) + \frac{\alpha_s N_c}{2\pi} \int_{1/sx_{10}^2}^{z'} \frac{dz''}{z''} \int_{1/z''s}^{\min\{x_{10}^2 z'/z'', 1/\Lambda^2\}} \frac{dx_{32}^2}{x_{32}^2} \left[3\tilde{G}(x_{32}^2, z''s) \right] \quad (76d)$$

$$+ \tilde{\Gamma}(x_{10}^2, x_{32}^2, z''s) + 2G_2(x_{32}^2, z''s) + \left(2 - \frac{N_f}{2N_c} \right) \Gamma_2(x_{10}^2, x_{32}^2, z''s) - \frac{N_f}{4N_c} \bar{\Gamma}(x_{10}^2, x_{32}^2, z''s) - \frac{N_f}{2N_c} \tilde{Q}(x_{32}^2, z''s)]$$

$$- \frac{\alpha_s N_f}{8\pi} \int_{\Lambda^2/s}^{z' x_{21}^2/x_{10}^2} \frac{dz''}{z''} \int_{\max\{x_{10}^2, 1/z''s\}}^{\min\{z/x_{10}^2, 1/\Lambda^2\}} \frac{dx_{32}^2}{x_{32}^2} [Q(x_{32}^2, z''s) + 2G_2(x_{32}^2, z''s)],$$

$$G_2(x_{10}^2, zs) = G_2^{(0)}(x_{10}^2, zs) + \frac{\alpha_s N_c}{\pi} \int_{\frac{\Lambda^2}{s}}^z \frac{dz'}{z'} \int_{\max\{x_{10}^2, \frac{1}{z's}\}}^{\min\{\frac{z}{z'}, x_{10}^2, 1/\Lambda^2\}} \frac{dx_{21}^2}{x_{21}^2} \left[\tilde{G}(x_{21}^2, z's) + 2G_2(x_{21}^2, z's) \right], \quad (76e)$$

$$\Gamma_2(x_{10}^2, x_{21}^2, z's) = G_2^{(0)}(x_{10}^2, z's) + \frac{\alpha_s N_c}{\pi} \int_{\frac{\Lambda^2}{s}}^z \frac{dz''}{z''} \int_{\max\{x_{10}^2, \frac{1}{z's}\}}^{\min\{\frac{z'}{z''}, x_{21}^2, 1/\Lambda^2\}} \frac{dx_{32}^2}{x_{32}^2} \left[\tilde{G}(x_{32}^2, z''s) + 2G_2(x_{32}^2, z''s) \right], \quad (76f)$$

$$\tilde{Q}(x_{10}^2, zs) = \tilde{Q}^{(0)}(x_{10}^2, zs) - \frac{\alpha_s N_c}{2\pi} \int_{\frac{\Lambda^2}{s}}^z \frac{dz'}{z'} \int_{\max\{x_{10}^2, \frac{1}{z's}\}}^{\min\{\frac{z}{z'}, x_{10}^2, 1/\Lambda^2\}} \frac{dx_{21}^2}{x_{21}^2} [Q(x_{21}^2, z's) + 2G_2(x_{21}^2, z's)]. \quad (76g)$$

$$\alpha = A^+, \quad \beta = F^{12}$$

Helicity JIMWLK

$$\langle \mathcal{O}_{\alpha,\beta,\psi,\bar{\psi}} \rangle_Y = \frac{\int \mathcal{D}\alpha \mathcal{D}\beta \mathcal{D}\psi \mathcal{D}\bar{\psi} \mathcal{O}_{\alpha,\beta,\psi,\bar{\psi}} \mathcal{W}_Y[\alpha,\beta,\psi,\bar{\psi}]}{\int \mathcal{D}\alpha \mathcal{D}\beta \mathcal{D}\psi \mathcal{D}\bar{\psi} \mathcal{W}_Y[\alpha,\beta,\psi,\bar{\psi}]}$$

- To go beyond the large- N_c and large- $N_c \& N_f$ limits need to write down a helicity analogue of JIMWLK evolution.
- This has been done in F. Cougoulic, YK, arXiv:1910.04268 [hep-ph], arXiv:2005.14688 [hep-ph]):

$$W_\tau[\alpha, \beta, \psi, \bar{\psi}] = W_\tau^{(0)}[\alpha, \beta, \psi, \bar{\psi}] + \int d^3\tau' \mathcal{K}_h[\tau, \tau'] \cdot W_{\tau'}[\alpha, \beta, \psi, \bar{\psi}]$$

with $\tau \equiv \{z, z X_\perp^2, z Y_\perp^2\}$ and the kernel

$$\begin{aligned} \mathcal{K}_h[\tau, \tau'] &= \frac{\alpha_s}{\pi^2} \int d^2 w_\perp \frac{\underline{X}' \cdot \underline{Y}'}{X'^2 Y'^2} \theta^{(3)}(\tau - \tau') \theta\left(z' - \frac{\Lambda^2}{s}\right) \theta\left(X'^2 - \frac{1}{z' s}\right) \theta\left(Y'^2 - \frac{1}{z' s}\right) \xrightarrow{\text{Life-time ordered!}} \\ &\times \left\{ U_w^{ba} D_{x,a,<}^+ D_{y,b,>}^+ - \frac{1}{2} (D_{x,a,<}^+ D_{y,a,<}^+ + D_{x,a,>}^+ D_{y,a,>}^+) \right. \\ &+ \frac{1}{2} U_w^{pol,ba} (D_{x,a,<}^+ D_{y,b,>}^\perp + D_{x,a,<}^\perp D_{y,b,>}^+) \quad \text{Regular (spin-averaged) JIMWLK} \\ &+ \left. \left(\frac{1}{2} \gamma^5 \gamma^- \right)_{\beta\alpha} \frac{1}{2} \left((V_w^{pol})_{ij} D_{x,j,\alpha,<}^\psi D_{y,i,\beta,>}^\psi + (V_w^{pol\dagger})_{ij} D_{x,j,\alpha,>}^\bar{\psi} D_{y,i,\beta,<}^\psi \right) \right\} \quad \text{Polarized gluon emissions} \\ &\quad \text{Polarized quark emissions} \end{aligned}$$

Warning: the equation is incomplete, need to add other sub-eikonal corrections (a la our '22 & '24 papers)!

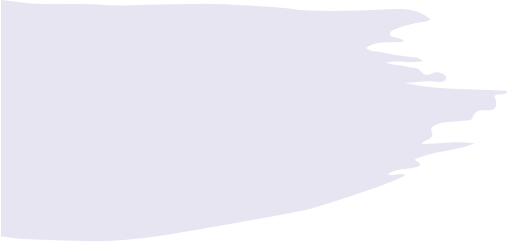
Helicity McLerran-Venugopalan Model

- The initial conditions for helicity JIMWLK are given by the helicity MV model, with the weight functional (F. Cougoulic, YK, 2005.14688 [hep-ph])

Standard MV

$$\begin{aligned} \mathcal{W}^{(0)}[\alpha, \beta, \psi, \bar{\psi}] &\propto \exp \left\{ - \int d^2x_\perp dx^- \operatorname{tr} \left[(\nabla_\perp^2 \alpha)^2 \frac{\mu_+^2 + \mu_-^2}{8\mu_+^2 \mu_-^2} + (\langle p^+ \rangle \beta)^2 \frac{\mu_+^2 + \mu_-^2}{2\mu_+^2 \mu_-^2} + (\nabla_\perp^2 \alpha) \langle p^+ \rangle \beta \frac{\mu_+^2 - \mu_-^2}{2\mu_+^2 \mu_-^2} \right] \right\} \\ &\times \exp \left\{ \int d^2x_\perp dx^- \langle p^+ \rangle \left[\frac{\nu_+^2 + \nu_-^2}{\nu_+^2 \nu_-^2} \bar{\psi} \frac{1}{2} \gamma^+ \nabla_\perp^2 \psi - \frac{\nu_+^2 - \nu_-^2}{\nu_+^2 \nu_-^2} \bar{\psi} \frac{1}{2} \gamma^+ \gamma^5 \nabla_\perp^2 \psi \right] \right\}. \end{aligned}$$

- Here $\alpha = A^+$, $\beta = F^{12}$
- The parameters μ_\pm , ν_\pm are \sim “saturation scales” of helicity-plus and helicity-minus partons.



Polarized DIS and SIDIS data analysis

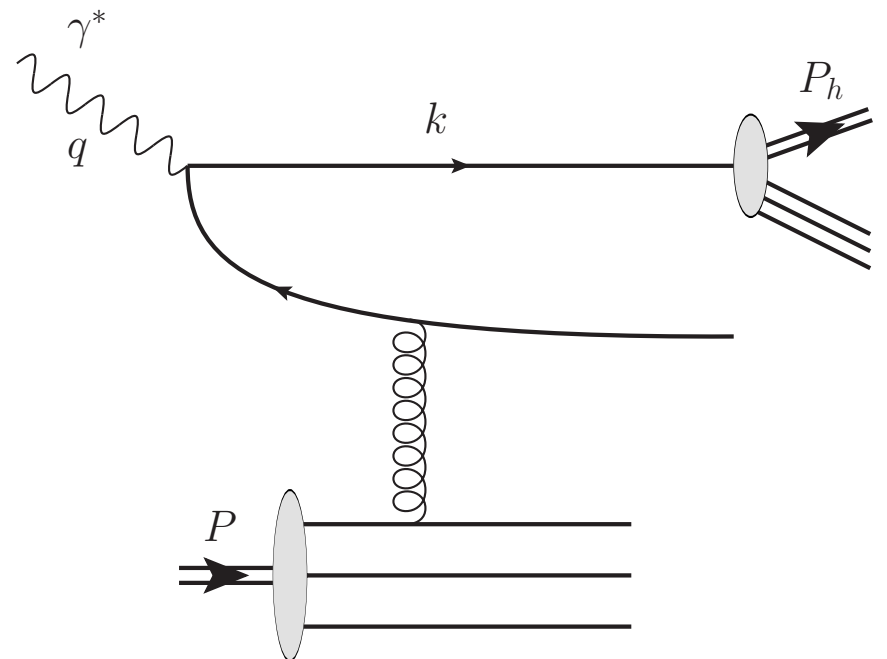
Polarized SIDIS at small x

Consider (anti-)quark production in the current fragmentation region in the polarized e+p scattering at small x.

The process is similar to the g_1 structure function calculation.

A straightforward calculation yields the SIDIS structure function (D_1 = fragmentation function)

$$g_1^h(x, z, Q^2) \approx \frac{1}{2} \sum_{q, \bar{q}} e_q^2 \Delta q(x, Q^2) D_1^{h/q}(z, Q^2)$$



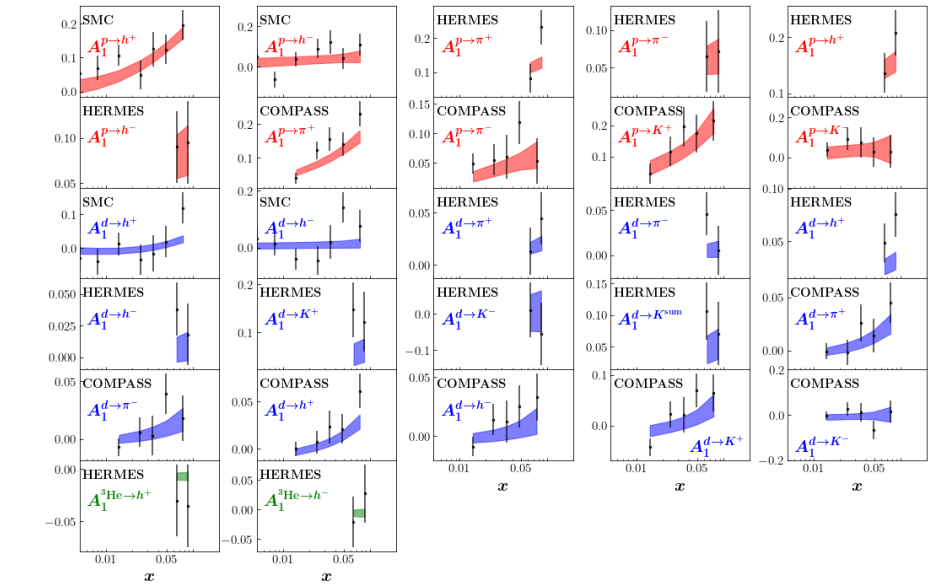
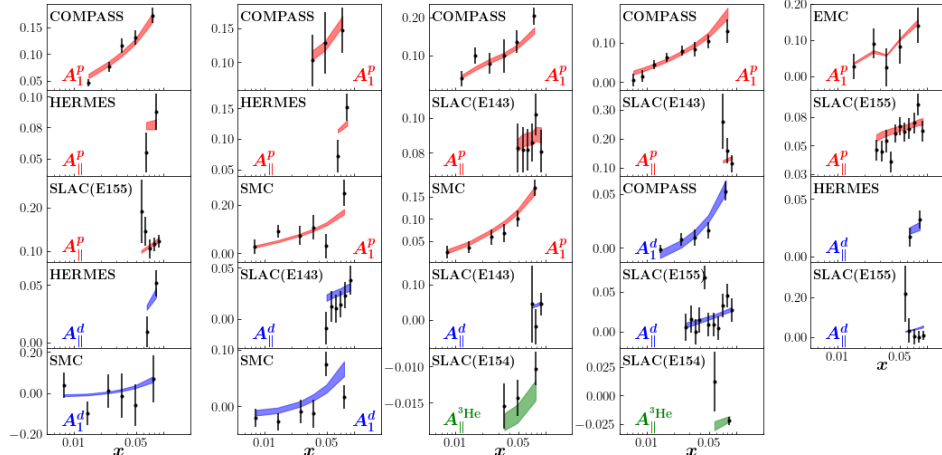
JAMsmallx: **Adamiak**, Baldonado, YK, Melnitchouk, Pitonyak, Sato, Sievert, Tarasov, Tawabutr,
2308.07461 [hep-ph]

$$5 \times 10^{-3} < x < 0.1 \equiv x_0$$

The analysis

$$1.69 \text{ GeV}^2 < Q^2 < 10.4 \text{ GeV}^2$$

Initial conditions: $Q^{(0)}(x_{10}^2, z_s) \sim G_2^{(0)}(x_{10}^2, z_s) \sim a \ln \frac{z_s}{\Lambda^2} + b \ln \frac{1}{x_{10}^2 \Lambda^2} + c$



$$A_{\parallel} = \frac{\sigma_{\downarrow\uparrow} - \sigma_{\uparrow\uparrow}}{\sigma_{\downarrow\uparrow} + \sigma_{\uparrow\uparrow}}$$

$$A_1 \approx \frac{g_1}{F_1}$$

$$A_{\parallel} \approx D A_1$$

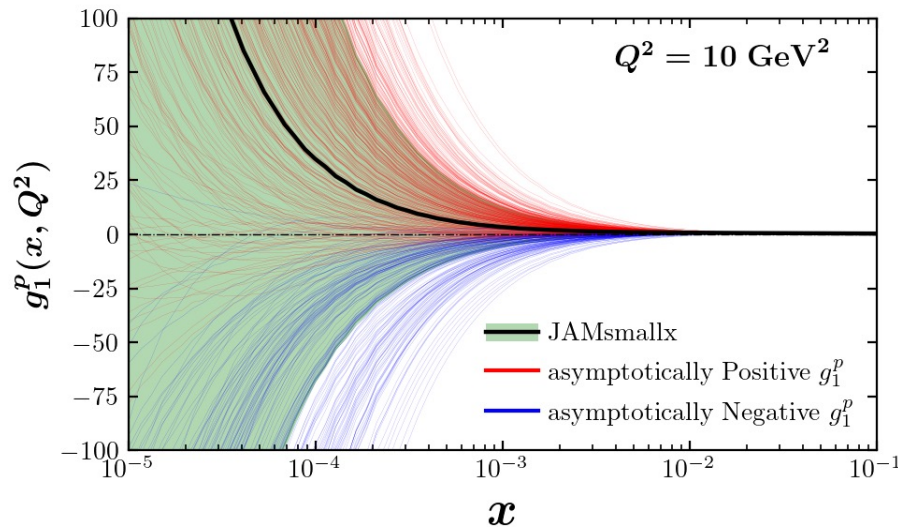
Double-spin asymmetries for p, d, and ${}^3\text{He}$

D= kinematic factor (known)

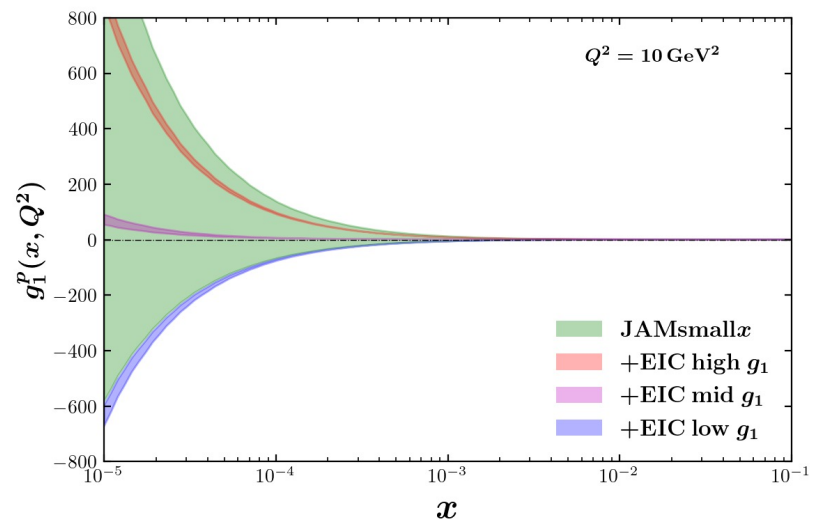
Running-coupling large- N_c & N_f evolution, 226 polarized DIS and SIDIS data points.

Proton g_1 structure function

JAM-smallx



g_1^p extracted from the existing data

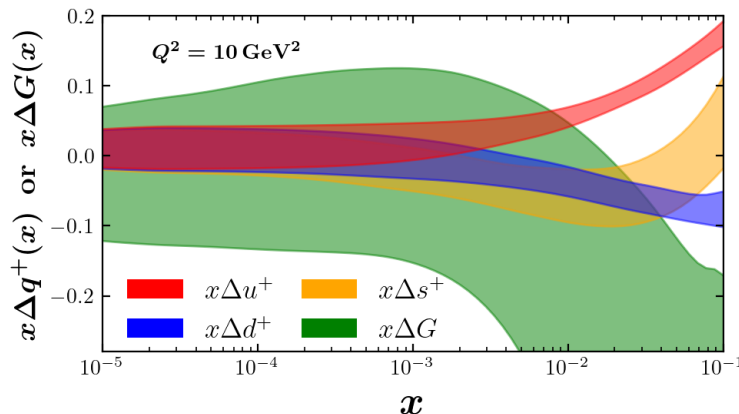


EIC impact

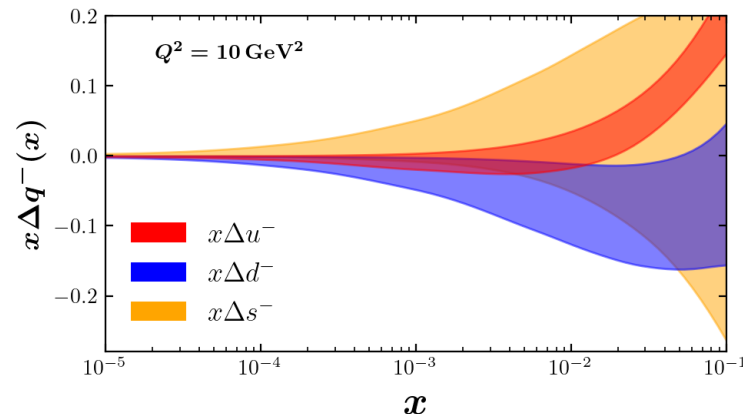
- JAM is based on a Bayesian Monte-Carlo: it uses replicas.
- Due to the lack of constraints, the spread is large.
- On the right, extraction using EIC pseudo-data (3 thin bands = 3 possible EIC data sets).

Helicity PDFs:

JAM-smallx

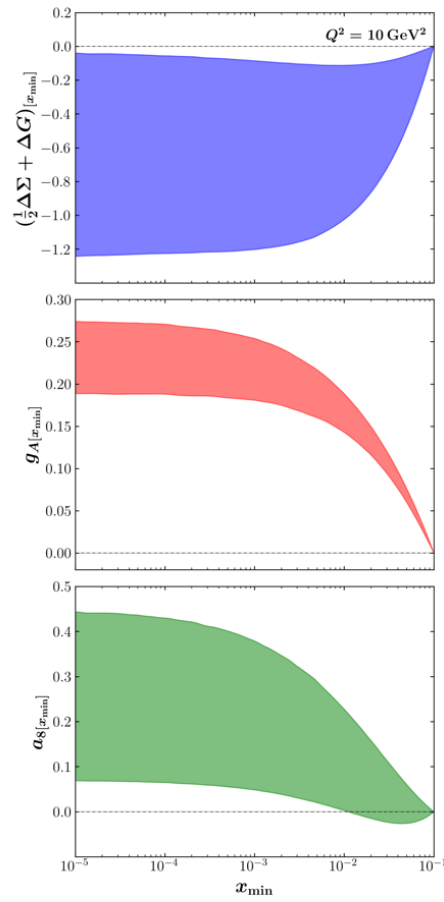
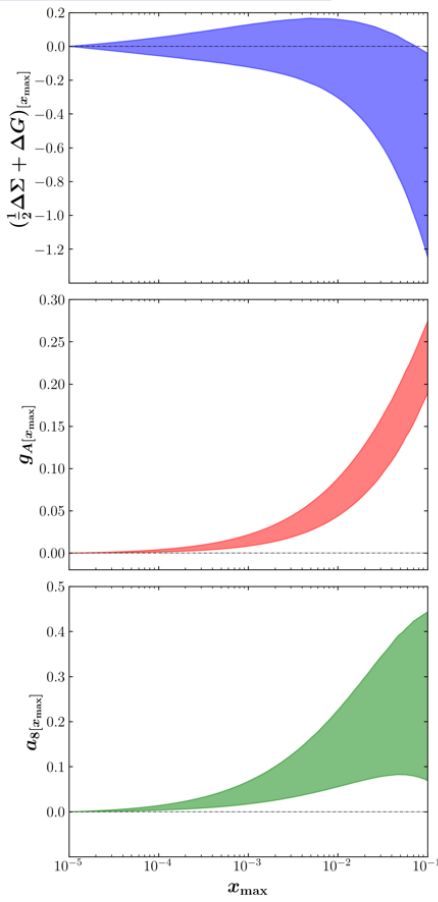


$$\Delta q^+ = \Delta q + \Delta \bar{q} \quad \Delta q^- = \Delta q - \Delta \bar{q}$$



Uncertainties at small x seem to be driven by our inability to constrain the dipole amplitude G_2 and G_{ilde} using the current data.

How much spin is there at small x?

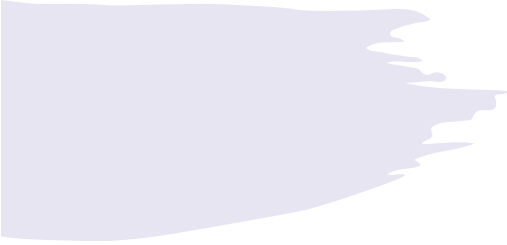


$$\begin{aligned} \left(\frac{1}{2} \Delta\Sigma + \Delta G \right)_{[x_{\min}]} (Q^2) &\equiv \int_{x_{\min}}^{x_0} dx \left(\frac{1}{2} \Delta\Sigma + \Delta G \right) (x, Q^2), \\ g_{A[x_{\min}]} (Q^2) &\equiv \int_{x_{\min}}^{x_0} dx [\Delta u^+(x, Q^2) - \Delta d^+(x, Q^2)], \\ a_{8[x_{\min}]} (Q^2) &\equiv \int_{x_{\min}}^{x_0} dx [\Delta u^+(x, Q^2) + \Delta d^+(x, Q^2) - 2 \Delta s^+(x, Q^2)] \\ \left(\frac{1}{2} \Delta\Sigma + \Delta G \right)_{[x_{\max}]} (Q^2) &\equiv \int_{10^{-5}}^{x_{\max}} dx \left(\frac{1}{2} \Delta\Sigma + \Delta G \right) (x, Q^2), \\ g_{A[x_{\max}]} (Q^2) &\equiv \int_{10^{-5}}^{x_{\max}} dx [\Delta u^+(x, Q^2) - \Delta d^+(x, Q^2)], \\ a_{8[x_{\max}]} (Q^2) &\equiv \int_{10^{-5}}^{x_{\max}} dx [\Delta u^+(x, Q^2) + \Delta d^+(x, Q^2) - 2 \Delta s^+(x, Q^2)] \end{aligned}$$

$$0.1 \int_{10^{-5}} dx \left(\frac{1}{2} \Delta\Sigma + \Delta G \right) (x) = -0.64 \pm 0.60$$

Negative net spin at small x!

Potentially a lot of spin at small x. However, the uncertainties are large. Need a way to constrain the initial conditions. To do so, we will include the polarized p+p data from RHIC.

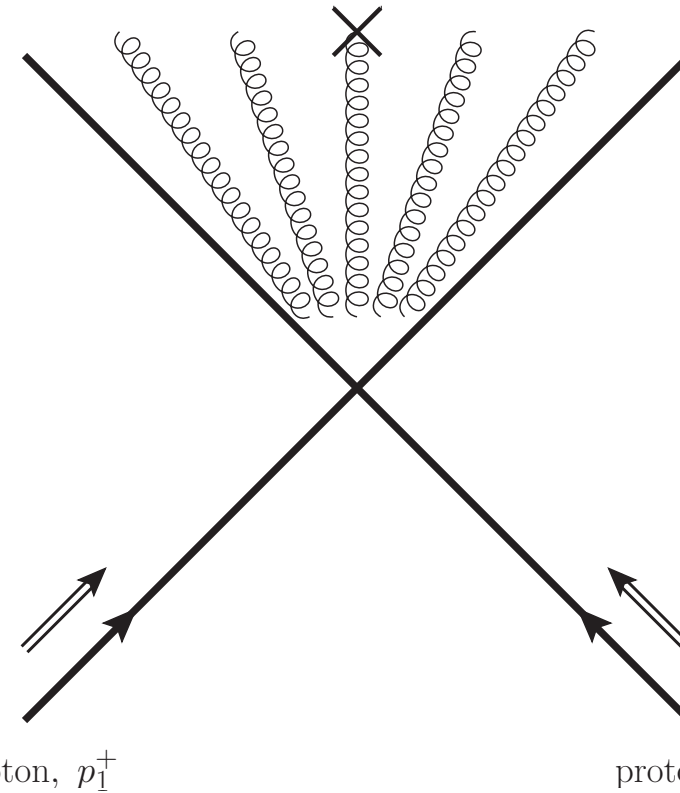


Particle production in polarized p+p collisions

YK, M. Li, 2403.06959 [hep-ph]

Gluon production at mid-rapidity

$$k^\mu = (k_T e^y / \sqrt{2}, k_T e^{-y} / \sqrt{2}, \vec{k}_T)$$



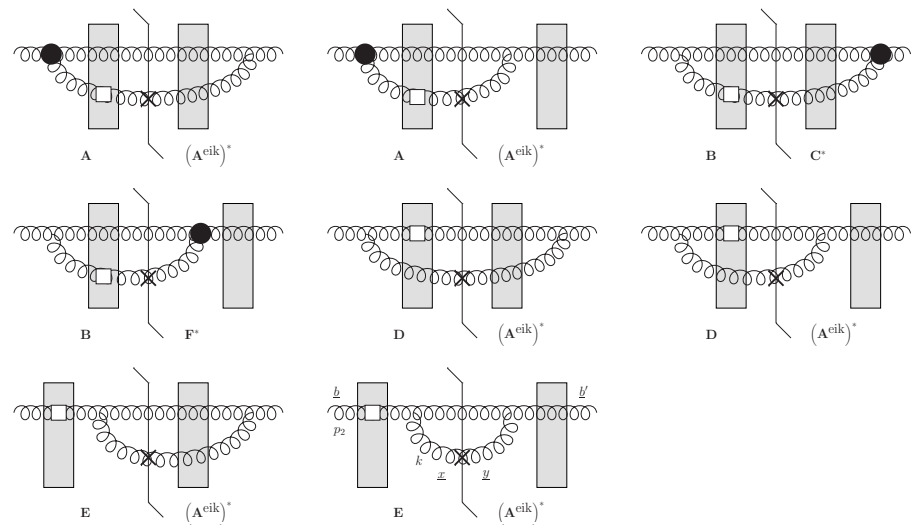
- We want to calculate gluon production cross section in polarized p+p collisions at mid-rapidity, where the gluon is small-x in both proton's wave functions.

Gluon production in polarized p+p collisions

Working in the shock wave picture, we first need to sum up the following diagrams (emission inside shock wave is suppressed by a log):

The result is shown below, and is cross-checked against the existing lowest-order calculations.

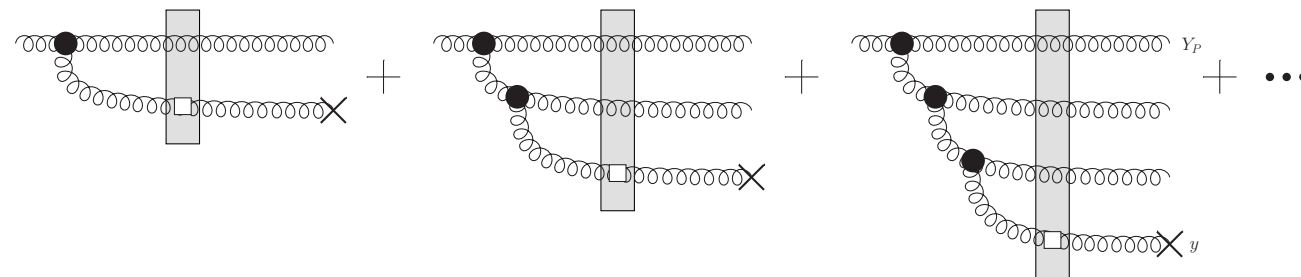
Only terms proportional to both protons' polarizations, $\sigma_1 \sigma_2$, are included.



$$\frac{d\sigma(\lambda)}{d^2k_T dy} = \lambda \frac{\alpha_s}{\pi^4} \frac{1}{s} N_c \int d^2x d^2y d^2b e^{-i\underline{k}\cdot(\underline{x}-\underline{y})} \left\{ \frac{\underline{x}-\underline{b}}{|\underline{x}-\underline{b}|^2} \cdot \frac{\underline{y}-\underline{b}}{|\underline{y}-\underline{b}|^2} \left[G_{\underline{x},\underline{y}}^{\text{adj}}(2k^- p_1^+) - G_{\underline{x},\underline{b}}^{\text{adj}}(2k^- p_1^+) \right. \right. \\ \left. \left. - \frac{1}{4} \left(G_{\underline{b},\underline{y}}^{\text{adj}}(2k^- p_1^+) + G_{\underline{b},\underline{x}}^{\text{adj}}(2k^- p_1^+) - 2 G_{\underline{b},\underline{b}'}^{\text{adj}}(2k^- p_1^+) \right) \right] - 2i k^i \frac{\underline{x}-\underline{b}}{|\underline{x}-\underline{b}|^2} \times \frac{\underline{y}-\underline{b}}{|\underline{y}-\underline{b}|^2} G_{\underline{x},\underline{b}}^{i \text{ adj}}(2k^- p_1^+) \right\}$$

Including small-x evolution

- We need to include small-x evolution on the projectile and target sides.
- This is simple on the target side, less so on the projectile side:



- We symmetrize the above expression with respect to target—projectile interchange, after which we can include the evolution on the projectile side as well.

Gluon production in polarized p+p collisions at mid-rapidity: the final result

- In the end we get the following expression for the cross section (at large N_c), where the dipole amplitudes Q and G_2 evolve via the above evolution equations (YK, M. Li, 2024):

$$\frac{d\sigma}{d^2 k_T dy} = \frac{C_F}{\alpha_s \pi^4} \frac{1}{s k_T^2} \int d^2 x e^{-ik \cdot x} \\ \times (4 Q_P - 2 G_{2P}) (x_\perp^2, \sqrt{2} p_2^- k_T e^{-y}) \begin{pmatrix} \frac{1}{4} \vec{\nabla}_\perp \cdot \vec{\nabla}_\perp & \vec{\nabla}_\perp^2 + \vec{\nabla}_\perp \cdot \vec{\nabla}_\perp \\ \vec{\nabla}_\perp^2 + \vec{\nabla}_\perp \cdot \vec{\nabla}_\perp & 0 \end{pmatrix} \begin{pmatrix} 4 Q_T \\ 2 G_{2T} \end{pmatrix} (x_\perp^2, \sqrt{2} p_1^+ k_T e^y).$$

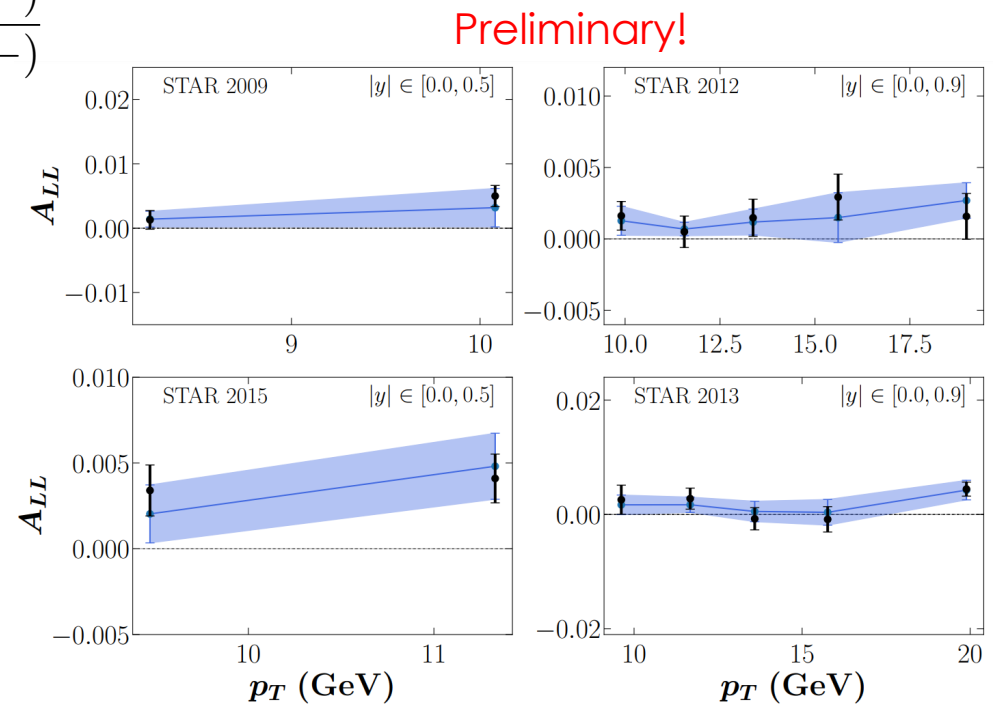
- Equivalently, in momentum space we obtain the following factorized expression in terms of TMDs (ΔH_{3L}^\perp is a twist-3 helicity-flip TMD):

$$\frac{d\sigma}{d^2 k_T dy} = -\frac{32\pi^4 \alpha_s}{N_c} \frac{1}{s k_T^2} \int \frac{d^2 q}{(2\pi)^2} \\ \times \begin{pmatrix} \Delta H_{3L}^{\perp dip P} & g_{1L}^{G dip P} \end{pmatrix} \left(q_T^2, \frac{k_T}{\sqrt{2} p_2^-} e^y \right) \begin{pmatrix} \underline{q} \cdot (\underline{k} - \underline{q}) & \underline{q} \cdot \underline{k} \\ \underline{k} \cdot (\underline{k} - \underline{q}) & 0 \end{pmatrix} \begin{pmatrix} \Delta H_{3L}^{\perp dip T} \\ g_{1L}^{G dip T} \end{pmatrix} \left((\underline{k} - \underline{q})^2, \frac{k_T}{\sqrt{2} p_1^+} e^{-y} \right)$$

Polarized p+p collisions: small-x phenomenology

$$A_{LL} = \frac{d\sigma(++) - d\sigma(+-)}{d\sigma(++) + d\sigma(+-)}$$

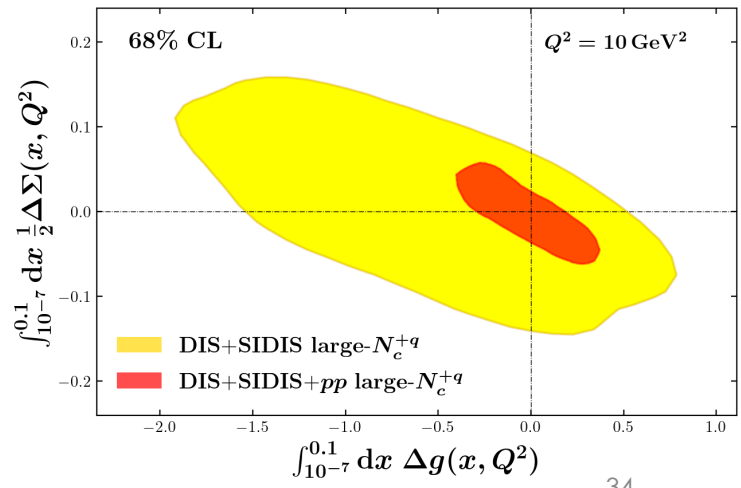
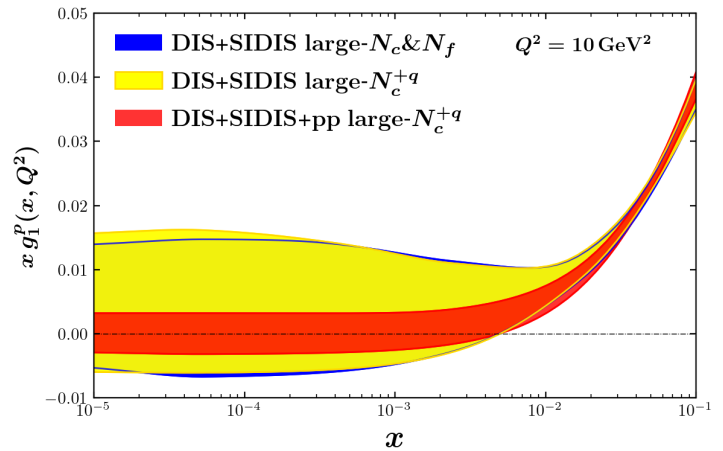
- The above result can be applied to RHIC data on jets' A_{LL} (JAMsmallx: D. Adamiak, **N. Baldonado**, et al, in preparation):
- Note that the calculation was for **gluons only**, quarks need to be included (in progress). Hence, comparison with the data is a proof-of-concept at this point.
- Only large- N_c evolution is employed with external quarks.

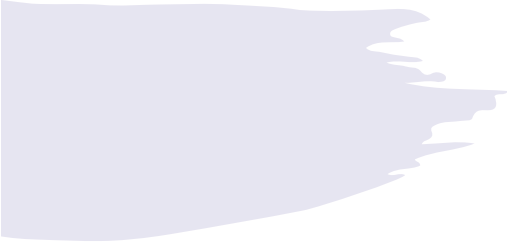


New constraints coming from polarized p+p data:

- Including more data constrains the initial conditions for the dipole amplitudes involved, resulting in more precise EIC predictions for the proton g_1 structure function and estimates of spin at low x :

Preliminary!

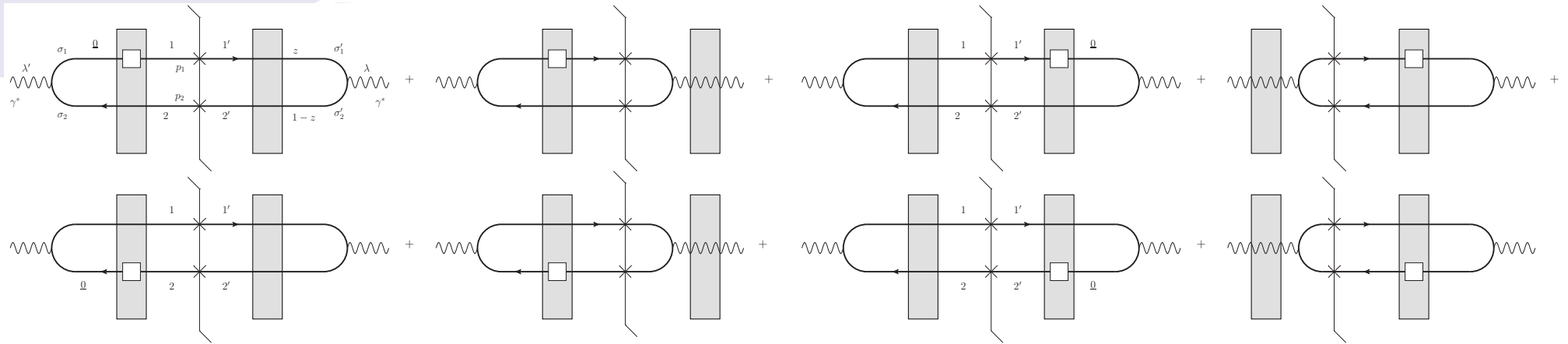




Inclusive dijet production in polarized e+p collisions

YK, M. Li, in preparation

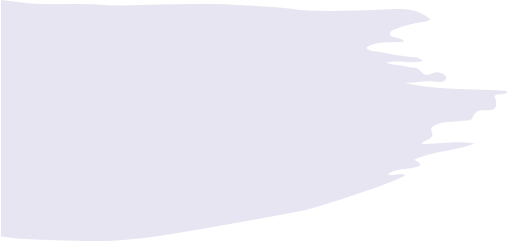
Inclusive dijet production in polarized e+p collisions



Consider double spin asymmetry (DSA) in inclusive dijet production in e+p collisions. In the b2b limit ($p_T \sim Q \gg \Delta_\perp \sim \Lambda_{QCD}$) the cross section probes the WW gluon helicity TMD (cf. F. Dominguez, B.-W. Xiao, and F. Yuan, 2010; F. Dominguez, C. Marquet, B.-W. Xiao, and F. Yuan, 2011, for unpolarized TMDs):

$$\sum_{\lambda=\pm 1} \lambda z(1-z) \frac{d\sigma_{\lambda\lambda}^{\gamma^* p \rightarrow q\bar{q}X}}{d^2 p d^2 \Delta dz} \approx -\frac{2 \alpha_s \alpha_{EM} Z_f^2}{s} [z^2 + (1-z)^2] \frac{p_T^2 - a_f^2}{(p_T^2 + a_f^2)^2} g_{1L}^{GWW} \left(x \approx \frac{p_T^2}{s}, \Delta_T^2 \right)$$

Since, in the linear regime, the two TMDs are the same, $g_{1L}^{GWW}(x, k_T^2) \approx g_{1L}^{Gdip}(x, k_T^2)$, we can use the future dijet data at EIC to further constrain gluon helicity distribution. $a_f^2 = Q^2 z(1-z) + m_f^2$



Elastic dijet production in polarized e+p collisions

YK, B. Manley, 2410.21260 [hep-ph]

OAM Distributions

- Let us write the (Jaffe-Manohar) quark and gluon OAM in terms of the Wigner distribution as

$$L_z = \int \frac{d^2 b_\perp db^- d^2 k_\perp dk^+}{(2\pi)^3} (\underline{b} \times \underline{k})_z W(k, b)$$

- After much algebra, we arrive at the quark and gluon OAM distributions at small x :

$$L_{q+\bar{q}}(x, Q^2) = \frac{N_c N_f}{2\pi^3} \int_{\Lambda^2/s}^1 \frac{dz}{z} \int_{\max\left\{\frac{1}{zs}, \frac{1}{Q^2}\right\}}^{\min\left\{\frac{1}{zQ^2}, \frac{1}{\Lambda^2}\right\}} \frac{dx_{10}^2}{x_{10}^2} \left[Q(x_{10}^2, zs) - 3G_2(x_{10}^2, zs) - I_3(x_{10}^2, zs) - 2I_4(x_{10}^2, zs) + I_5(x_{10}^2, zs) + 3I_6(x_{10}^2, zs) \right]$$

$$L_G(x, Q^2) = -\frac{2 N_c}{\alpha_s \pi^2} \left\{ \left[2 + 6x_{10}^2 \frac{\partial}{\partial x_{10}^2} + 2x_{10}^4 \frac{\partial^2}{\partial (x_{10}^2)^2} \right] [I_4(x_{10}^2, zs) + I_5(x_{10}^2, zs)] + \left[1 + x_{10}^2 \frac{\partial}{\partial x_{10}^2} \right] [I_5(x_{10}^2, zs) + I_6(x_{10}^2, zs)] \right\}_{x_{10}^2=1/Q^2, zs=Q^2/x}$$

OAM Distributions and Moment Amplitudes

$$L_{q+\bar{q}}(x, Q^2) = \frac{N_c N_f}{2\pi^3} \int_{\Lambda^2/s}^1 \frac{dz}{z} \int_{\max\left\{\frac{1}{zs}, \frac{1}{Q^2}\right\}}^{\min\left\{\frac{1}{zQ^2}, \frac{1}{\Lambda^2}\right\}} \frac{dx_{10}^2}{x_{10}^2} \left[Q(x_{10}^2, zs) - 3G_2(x_{10}^2, zs) - I_3(x_{10}^2, zs) \right. \\ \left. - 2I_4(x_{10}^2, zs) + I_5(x_{10}^2, zs) + 3I_6(x_{10}^2, zs) \right]$$

$$L_G(x, Q^2) = -\frac{2N_c}{\alpha_s \pi^2} \left\{ \left[2 + 6x_{10}^2 \frac{\partial}{\partial x_{10}^2} + 2x_{10}^4 \frac{\partial^2}{\partial (x_{10}^2)^2} \right] [I_4(x_{10}^2, zs) + I_5(x_{10}^2, zs)] \right. \\ \left. + \left[1 + x_{10}^2 \frac{\partial}{\partial x_{10}^2} \right] [I_5(x_{10}^2, zs) + I_6(x_{10}^2, zs)] \right\}_{x_{10}^2=1/Q^2, zs=Q^2/x}$$

- Q and G_2 are the same as above. However, we also now have the impact parameter **moments of dipole amplitudes**, labeled I_3, I_4, I_5 and I_6 :

$$\int d^2x_1 x_1^i Q_{10}(zs) = x_{10}^i I_3(x_{10}^2, zs) + \dots, \quad \begin{array}{c} x_0 \xrightarrow{\hspace{1cm}} \frac{1-z}{z} \\ x_1 \xrightarrow{\hspace{1cm}} z \end{array} + \begin{array}{c} x_0 \xrightarrow{\hspace{1cm}} \\ x_1 \xrightarrow{\hspace{1cm}} \end{array}$$

$$\int d^2x_1 x_1^i G_{10}^j(zs) = \epsilon^{ij} x_{10}^2 I_4(x_{10}^2, zs) + \epsilon^{ik} x_{10}^k x_{10}^j I_5(x_{10}^2, zs) + \epsilon^{jk} x_{10}^k x_{10}^i I_6(x_{10}^2, zs) + \dots$$

Evolution for Moment Dipole Amplitudes

$$\begin{pmatrix} I_3 \\ I_4 \\ I_5 \\ I_6 \end{pmatrix} (x_{10}^2, z s) = \begin{pmatrix} I_3^{(0)} \\ I_4^{(0)} \\ I_5^{(0)} \\ I_6^{(0)} \end{pmatrix} (x_{10}^2, z s) + \frac{\alpha_s N_c}{4\pi} \int_{\frac{1}{s x_{10}^2}}^z \frac{dz'}{z'} \int_{\frac{1}{z' s}}^{\frac{x_{10}^2}{s x_{10}^2}} \frac{dx_{21}^2}{x_{21}^2} \begin{pmatrix} 2\Gamma_3 - 4\Gamma_4 + 2\Gamma_5 + 6\Gamma_6 - 2\Gamma_2 \\ 0 \\ 0 \\ 0 \end{pmatrix} (x_{10}^2, x_{21}^2, z' s)$$

Evolution equations for the moment amplitudes in DLA and at large N_c are derived in
 YK, B. Manley,
 2310.18404 [hep-ph].

They can be solved numerically (same ref)
 and analytically (B. Manley,
 2401.05508 [hep-ph])

$$+ \frac{\alpha_s N_c}{4\pi} \int_{\frac{1}{s x_{10}^2}}^z \frac{dz'}{z'} \int_{\max[x_{10}^2, \frac{1}{z' s}]}^{\min[\frac{z'}{z''} x_{10}^2, \frac{1}{\Lambda^2}]} \frac{dx_{21}^2}{x_{21}^2} \begin{pmatrix} 4 & -4 & 2 & 6 & -4 & -6 \\ 0 & 4 & 2 & -2 & 0 & 1 \\ -2 & 2 & -1 & -3 & 2 & 3 \\ 0 & 0 & 0 & 0 & 2 & 4 \end{pmatrix} \begin{pmatrix} I_3 \\ I_4 \\ I_5 \\ I_6 \\ G \\ G_2 \end{pmatrix} (x_{21}^2, z' s)$$

$$\begin{pmatrix} \Gamma_3 \\ \Gamma_4 \\ \Gamma_5 \\ \Gamma_6 \end{pmatrix} (x_{10}^2, x_{21}^2, z' s) = \begin{pmatrix} I_3^{(0)} \\ I_4^{(0)} \\ I_5^{(0)} \\ I_6^{(0)} \end{pmatrix} (x_{10}^2, z' s)$$

$$+ \frac{\alpha_s N_c}{4\pi} \int_{\frac{1}{s x_{10}^2}}^{z'} \frac{dz''}{z''} \int_{\frac{1}{z'' s}}^{\min[x_{10}^2, x_{21}^2, \frac{z'}{z''}]} \frac{dx_{32}^2}{x_{32}^2} \begin{pmatrix} 2\Gamma_3 - 4\Gamma_4 + 2\Gamma_5 + 6\Gamma_6 - 2\Gamma_2 \\ 0 \\ 0 \\ 0 \end{pmatrix} (x_{10}^2, x_{32}^2, z'' s)$$

$$+ \frac{\alpha_s N_c}{4\pi} \int_{\frac{1}{s x_{10}^2}}^{z' \frac{x_{21}^2}{x_{10}^2}} \frac{dz''}{z''} \int_{\max[x_{10}^2, \frac{1}{z'' s}]}^{\min[\frac{z'}{z''} x_{21}^2, \frac{1}{\Lambda^2}]} \frac{dx_{32}^2}{x_{32}^2} \begin{pmatrix} 4 & -4 & 2 & 6 & -4 & -6 \\ 0 & 4 & 2 & -2 & 0 & 1 \\ -2 & 2 & -1 & -3 & 2 & 3 \\ 0 & 0 & 0 & 0 & 2 & 4 \end{pmatrix} \begin{pmatrix} I_3 \\ I_4 \\ I_5 \\ I_6 \\ G \\ G_2 \end{pmatrix} (x_{32}^2, z'' s)$$

Two intercepts, again

- The evolution equations for moment dipole amplitudes have been solved analytically by B. Manley in 2401.05508 [hep-ph]. The solution was constructed using the double Laplace transform, similar to the solution for the impact-parameter integrated amplitudes.
- The resulting small-x OAM asymptotics at large N_c is the same as for helicity PDFs,

$$L_{q+\bar{q}}(x, Q^2) \sim L_G(x, Q^2) \sim \left(\frac{1}{x}\right)^{\alpha_h}$$

with the intercept

$$\alpha_h = \frac{4}{3^{1/3}} \sqrt{\operatorname{Re} [(-9 + i\sqrt{111})^{1/3}]} \sqrt{\frac{\alpha_s N_c}{2\pi}} \approx 3.661 \sqrt{\frac{\alpha_s N_c}{2\pi}}$$

- This slightly disagrees with the work of Boussarie, Hatta, and Yuan (2019), which resulted in the same intercept as BER:

$$\alpha_h = \sqrt{\frac{17 + \sqrt{97}}{2}} \sqrt{\frac{\alpha_s N_c}{2\pi}} \approx 3.664 \sqrt{\frac{\alpha_s N_c}{2\pi}}$$

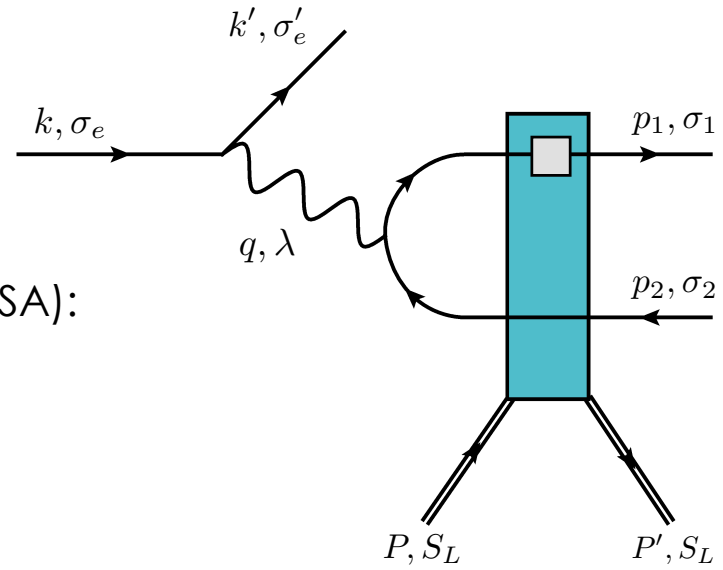
Elastic dijet production in e+p collisions

The process is similar to the one above, except now the proton remains intact.

One considers two observables, double spin asymmetry (DSA) and single spin asymmetry (SSA):

$$d\sigma^{DSA} = \frac{1}{4} \sum_{\sigma_e, S_L} \sigma_e S_L d\sigma(\sigma_e, S_L),$$

$$d\sigma^{SSA} = \frac{1}{4} \sum_{\sigma_e, S_L} S_L d\sigma(\sigma_e, S_L)$$



Measuring OAM distributions in elastic e+p collisions

- In the small-t limit (p_T , $Q \gg \Lambda_{QCD} \gg \Delta_\perp$ with $t = -\Delta_\perp^2$) the elastic dijet DSA measures moments of dipole amplitudes, thus **allowing (in principle) to measure OAM distributions!**
- Cf. Hatta et al, 2016; S. Bhattacharya, R. Boussarie and Y. Hatta, 2022 & 2024; S. Bhattacharya, D. Zheng and J. Zhou, 2023.
- Feasibility study in progress (G.Z. Becker, B. Manley, YK).

$$z(1-z) \frac{1}{2} \sum_{S_L, \lambda \pm 1} S_L \lambda \frac{d\sigma_{\text{symm.}}^{\gamma^* p \rightarrow q\bar{q}p'}}{d^2 p d^2 \Delta dz} = -\frac{2}{(2\pi)^5 z(1-z)s} \int d^2 x_{12} d^2 x_{1'2'} e^{-i\vec{p} \cdot (\underline{x}_{12} - \underline{x}_{1'2'})} N(x_{1'2'}^2, s) \quad (107a)$$

$$\begin{aligned} & \times \left\{ \left[\left(1 - 2z + i\Delta \cdot \underline{x}_{12} (z^2 + (1-z)^2) - \frac{i}{2} \Delta \cdot \underline{x}_{1'2'} (1-2z)^2 \right) Q(x_{12}^2, s) - i\Delta \cdot \underline{x}_{12} I_3(x_{12}^2, s) \right. \right. \\ & \quad \left. \left. - i\Delta \times \underline{x}_{12} J_3(x_{12}^2, s) \right] \Phi_{\text{TT}}^{[1]}(\underline{x}_{12}, \underline{x}_{1'2'}, z) \right. \\ & \quad \left. + \left[i(1-2z) \left(\Delta^j \epsilon^{ji} x_{12}^2 I_4(x_{12}^2, s) + \Delta \times \underline{x}_{12} x_{12}^i I_5(x_{12}^2, s) + \Delta^i x_{12}^2 J_4(x_{12}^2, s) + \Delta \cdot \underline{x}_{12} x_{12}^i J_5(x_{12}^2, s) \right) \right. \right. \\ & \quad \left. \left. - \left[1 + i(1-2z) \Delta \cdot \left(\underline{x}_{12} - \frac{\underline{x}_{1'2'}}{2} \right) \right] \left(\epsilon^{ik} x_{12}^k G_2(x_{12}^2, s) + x_{12}^i G_1(x_{12}^2, s) \right) \right] \right. \\ & \quad \left. \times \left(\partial_\perp^i - ip^i \right) \Phi_{\text{TT}}^{[2]}(\underline{x}_{12}, \underline{x}_{1'2'}, z) \right\} + \mathcal{O}(\Delta_\perp^2), \end{aligned}$$

$$z(1-z) \frac{1}{2} \sum_{S_L, \lambda \pm 1} S_L \left[e^{i\lambda\phi} \frac{d\sigma_{\text{symm.}}^{\gamma^* p \rightarrow q\bar{q}p'}}{d^2 p d^2 \Delta dz} + \text{c.c.} \right] = -\frac{2i\sqrt{2}}{2(2\pi)^5 z(1-z)s} \int d^2 x_{12} d^2 x_{1'2'} e^{-i\vec{p} \cdot (\underline{x}_{12} - \underline{x}_{1'2'})} \quad (107b)$$

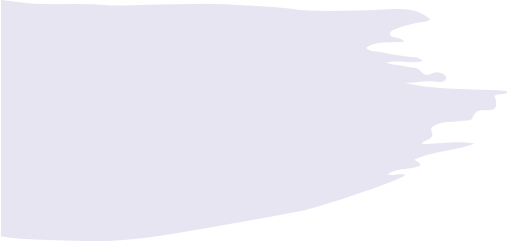
$$\begin{aligned} & \times N(x_{1'2'}^2, s) \left\{ \left[\left(1 - 2z + i\Delta \cdot \underline{x}_{12} (z^2 + (1-z)^2) - \frac{i}{2} \Delta \cdot \underline{x}_{1'2'} (1-2z)^2 \right) Q(x_{12}^2, s) - i\Delta \cdot \underline{x}_{12} I_3(x_{12}^2, s) \right. \right. \\ & \quad \left. \left. - i\Delta \times \underline{x}_{12} J_3(x_{12}^2, s) \right] \left[\frac{\hat{k} \cdot \underline{x}_{12}}{x_{12}} \Phi_{\text{LT}}^{[1]}(\underline{x}_{12}, \underline{x}_{1'2'}, z) - \frac{\hat{k} \cdot \underline{x}_{1'2'}}{x_{1'2'}} \Phi_{\text{LT}}^{[1]}(\underline{x}_{1'2'}, \underline{x}_{12}, z) \right] \right. \\ & \quad \left. + \left[i(1-2z) \left(\Delta^j \epsilon^{ji} x_{12}^2 I_4(x_{12}^2, s) + \Delta \times \underline{x}_{12} x_{12}^i I_5(x_{12}^2, s) + \Delta^i x_{12}^2 J_4(x_{12}^2, s) + \Delta \cdot \underline{x}_{12} x_{12}^i J_5(x_{12}^2, s) \right) \right. \right. \\ & \quad \left. \left. - \left[1 + i(1-2z) \Delta \cdot \left(\underline{x}_{12} - \frac{\underline{x}_{1'2'}}{2} \right) \right] \left(\epsilon^{ik} x_{12}^k G_2(x_{12}^2, s) + x_{12}^i G_1(x_{12}^2, s) \right) \right] \right. \\ & \quad \left. \times \left(\partial_\perp^i - ip^i \right) \left[\frac{\hat{k} \times \underline{x}_{12}}{x_{12}} \Phi_{\text{LT}}^{[2]}(\underline{x}_{12}, \underline{x}_{1'2'}, z) + \frac{\hat{k} \times \underline{x}_{1'2'}}{x_{1'2'}} \Phi_{\text{LT}}^{[2]}(\underline{x}_{1'2'}, \underline{x}_{12}, z) \right] \right\} + \mathcal{O}(\Delta_\perp^2), \end{aligned}$$

Conclusions

- The small- x helicity formalism in the double logarithmic approximation (DLA) + running coupling allows to do successful polarized DIS + SIDIS phenomenology based on the existing small- x data.
- However, the multitude of different dipole amplitudes in the formalism prevents precise EIC predictions: there are too many dipole amplitudes, making their initial conditions hard to fix using the existing data.
- Polarized p+p data on A_{LL} from RHIC, if properly included, may help. The first step in this direction is presented above.
- When EIC comes online, DSA in inclusive dijet production would help constrain gluon helicity distributions.
- Elastic dijets at EIC may help us measure the OAM distributions as well (and compare their x -dependence to theory).



Happy Birthday Edmond!



Backup slides

Small-x Asymptotics for Helicity Distributions

- Let's take a closer look at the anomalous dimension:

$$\Delta G(x, Q^2) = \int \frac{d\omega}{2\pi i} \left(\frac{1}{x}\right)^\omega \left(\frac{Q^2}{\Lambda^2}\right)^{\Delta\gamma_{GG}(\omega)} \Delta G_\omega(\Lambda^2)$$

- In the pure-glue case, Bartels, Ermolaev and Ryskin's (BER) anomalous dimension can be found analytically. It reads (KPS '16)

$$\Delta\gamma_{GG}^{BER}(\omega) = \frac{1}{2} \left[\omega - \sqrt{\omega^2 - 16 \bar{\alpha}_s \frac{1 - \frac{3\bar{\alpha}_s}{\omega^2}}{1 - \frac{\bar{\alpha}_s}{\omega^2}}} \right] \quad \bar{\alpha}_s = \frac{\alpha_s N_c}{2\pi}$$

- Our evolution's anomalous dimension can be found analytically at large- N_c (J. Borden, YK, 2304.06161 [hep-ph]):

$$\Delta\gamma_{GG}^{us}(\omega) = \frac{1}{2} \left[\omega - \sqrt{\omega^2 - 16 \bar{\alpha}_s \sqrt{1 - \frac{4\bar{\alpha}_s}{\omega^2}}} \right]$$

A Tale of Two Anomalous Dimensions

- The two anomalous dimensions look similar but are not the same function.

$$\Delta\gamma_{GG}^{BER}(\omega) = \frac{1}{2} \left[\omega - \sqrt{\omega^2 - 16 \bar{\alpha}_s \frac{1 - \frac{3\bar{\alpha}_s}{\omega^2}}{1 - \frac{\bar{\alpha}_s}{\omega^2}}} \right] \quad \Delta\gamma_{GG}^{us}(\omega) = \frac{1}{2} \left[\omega - \sqrt{\omega^2 - 16 \bar{\alpha}_s \sqrt{1 - \frac{4\bar{\alpha}_s}{\omega^2}}} \right]$$

- Their expansions in α_s start out the same, then **differ at four (!) loops** (the first 3 terms agree with the existing finite-order calculations, the four-loop result is unknown):

$$\Delta\gamma_{GG}^{BER}(\omega) = \frac{4\bar{\alpha}_s}{\omega} + \frac{8\bar{\alpha}_s^2}{\omega^3} + \frac{56\bar{\alpha}_s^3}{\omega^5} + \frac{504\bar{\alpha}_s^4}{\omega^7} + \dots$$

$$\Delta\gamma_{GG}^{us}(\omega) = \frac{4\bar{\alpha}_s}{\omega} + \frac{8\bar{\alpha}_s^2}{\omega^3} + \frac{56\bar{\alpha}_s^3}{\omega^5} + \frac{496\bar{\alpha}_s^4}{\omega^7} + \dots$$

A Tale of Two Intercepts

$$\Delta G(x, Q^2) = \int \frac{d\omega}{2\pi i} \left(\frac{1}{x}\right)^\omega \left(\frac{Q^2}{\Lambda^2}\right)^{\Delta\gamma_{GG}(\omega)} \Delta G_\omega(\Lambda^2)$$

$$\Delta\gamma_{GG}^{BER}(\omega) = \frac{1}{2} \left[\omega - \sqrt{\omega^2 - 16 \bar{\alpha}_s \frac{1 - \frac{3\bar{\alpha}_s}{\omega^2}}{1 - \frac{\bar{\alpha}_s}{\omega^2}}} \right] \quad \Delta\gamma_{GG}^{us}(\omega) = \frac{1}{2} \left[\omega - \sqrt{\omega^2 - 16 \bar{\alpha}_s \sqrt{1 - \frac{4\bar{\alpha}_s}{\omega^2}}} \right]$$

- The intercept (largest power $\text{Re}[\omega]$) is given by the right-most singularity (branch point) of the anomalous dimension.

- For BER this gives $\alpha_h = \sqrt{\frac{17 + \sqrt{97}}{2}} \sqrt{\frac{\alpha_s N_c}{2\pi}} \approx 3.664 \sqrt{\frac{\alpha_s N_c}{2\pi}}$

- For us $\alpha_h = \frac{4}{3^{1/3}} \sqrt{\text{Re} [(-9 + i\sqrt{111})^{1/3}]} \sqrt{\frac{\alpha_s N_c}{2\pi}} \approx 3.661 \sqrt{\frac{\alpha_s N_c}{2\pi}}$

OAM Distribution to hPDF Ratios

- Following Boussarie *et al* (2019), we consider the ratios of OAM distributions to helicity PDFs at small x .
- For these ratios, Boussarie *et al*, predict, using the Wandzura-Wilczek approximation:

$$\frac{L_{q+\bar{q}}(x, Q^2)}{\Delta\Sigma(x, Q^2)} = -\frac{1}{1 + \alpha_h}$$

$$\frac{L_G(x, Q^2)}{\Delta G(x, Q^2)} = -\frac{2}{1 + \alpha_h}$$

$$\Delta\Sigma(x, Q^2) \Big|_{x \ll 1} \sim \Delta G(x, Q^2) \Big|_{x \ll 1} \sim \left(\frac{1}{x}\right)^{\alpha_h}$$

$$L_{q+\bar{q}}(x, Q^2) \sim L_G(x, Q^2) \sim \left(\frac{1}{x}\right)^{\alpha_h}$$

OAM Distribution to hPDF Ratios

- Analytic solution from B. Manley, 2401.05508 [hep-ph], gives

$$t = \sqrt{\frac{\alpha_s N_c}{2\pi} \ln \frac{Q^2}{\Lambda^2}}$$

$$\alpha_s = 0.25 \quad \Lambda = 1 \text{ GeV}$$

$$\frac{L_{q+\bar{q}}(x, Q^2)}{\Delta\Sigma(x, Q^2)} = -\frac{1}{1 + \alpha_h}$$

$$\frac{L_G(x, Q^2)}{\Delta G(x, Q^2)} = -\frac{2}{1 + \alpha_h}$$

